Journal of Functional Foods 72 (2020) 104045

Contents lists available at ScienceDirect

Journal of Functional Foods

journal homepage: www.elsevier.com/locate/jff

Bifidobacterium breve ATCC15700 pretreatment prevents alcoholic liver disease through modulating gut microbiota in mice exposed to chronic alcohol intake

Xiaozhu Tian[a], Rong Li[a], Yiming Jiang[b], Fei Zhao[c], Zhengsheng Yu[a], Yiqing Wang[d], Zixing Dong[e], Pu Liu[a,*], Xiangkai Li[a,*]

[a] Ministry of Education Key Laboratory of Cell Activities and Stress Adaptations, School of Life Science, Lanzhou University, Tianshui South Road #222, Lanzhou 730000, Gansu, PR China
[b] Institute of Virology (VIRO), Helmholtz Zentrum München, German Research Center for Environmental Health, Ingolstädter Landstr. 1, 85764 Neuherberg, Germany
[c] Medical College of Northwest Minzu University, Lanzhou, 730030, Gansu, PR China
[d] The Reproductive Medicine Special Hospital of the First Hospital of Lanzhou University, Lanzhou, Gansu, PR China
[e] Henan Provincial Engineering Laboratory of Insect Bio-reactor and Henan Key Laboratory of Ecological Security for Water Region of Mid-line of South-to-North, Nanyang Normal University, Nanyang 473061, Henan, PR China

ARTICLE INFO

Keywords:
Bifidobacterium breve ATCC15700
Alcoholic liver disease
Immune homeostasis
Inflammation
Intestinal barrier function
Gut microbiota

ABSTRACT

Gut microbiota has been identified as a key player in the development of alcoholic liver disease (ALD). Targeting gut microbiota with probiotic intervention will be an attractive approach to prevent ALD. Here, we investigated the effects of probiotic *Bifidobacterium breve* ATCC15700 (ATCC15700) on liver injury and gut microbiota in mice exposed to chronic alcohol intake. Our results showed that oral administration of ATCC15700 significantly decreased endotoxemia, maintained immune homeostasis, and alleviated alcohol-induced liver injury. ATCC15700 also promoted intestinal barrier function by enhancing the expressions of tight junction proteins in alcohol-treated mice. Moreover, analysis of gut microbiota showed that ATCC15700 normalized the structure and composition of the alcohol-disrupted gut microbiota. Correlation between gut microbiota and liver injury parameters revealed that specific bacteria, including *S24_7*, unclassified *Clostridiales*, *Butyricicoccus*, *Oscillospira*, *Ruminococcus*, *Mucispirillum* and unclassified *Lachnospiraceae*, were predominantly associated with ALD. In conclusion, ATCC15700 protected alcohol-exposed mice against liver injury via modulating gut micobiota.

1. Introduction

Alcoholic liver disease (ALD) caused by alcohol abuse is a leading cause of severe morbidity and mortality worldwide (Rehm, Samokhvalov, & Shield, 2013). Multiple factors participated in the pathogenesis of ALD, such as direct toxic effects of alcohol, oxidative stress, inflammation, intestinal permeability, and gut dysbiosis (Dunn & Shah, 2016). However, the molecular mechanisms involved in ALD are not well defined and need further investigations.

More than 90% of alcohol is absorbed in the intestine, and most of it is metabolized in the liver (Crabb, Matsumoto, Chang, & You, 2004). Therefore, alcohol-induced damage to the intestine and liver is direct. Alcohol and its metabolites acetaldehyde are able to directly disrupt intestinal tight junctions and impair hepatic proteins and DNA, resulting in hepatocyte injury (Basuroy, Sheth, Mansbach, & Rao, 2005; Leung & Nieto, 2013). However, there are only about 10–35% of heavy drinkers developing alcoholic steatohepatitis, of which approximately 10% develops into liver cirrhosis (Stickel, Moreno, Hampe, & Morgan, 2017). Although there may be individual differences, factors other than alcohol or acetaldehyde appear to be more associated with the pathogenesis of ALD, one of which has been identified as gut microbiota.

Accumulating evidence demonstrates that alcohol consumption

Abbreviations: PBS, phosphate-buffered saline; Alc, alcohol; TG, triacylglycerol; TNF, tumor necrosis factor; IL, interleukin; LPS, lipopolysaccharide; SOD, super oxide dismutase; GSH, glutathione; CAT, catalase; MDA, malondialdehyde; ALD, alcoholic liver disease; ROS, reactive oxygen species; CYP2E1, cytochrome P450 2E1; NF-κB, nuclear factor-κB; TLR, Toll-like receptor; ALT, alanine aminotransferase; AST, aspartate aminotransferase; ELISA, enzyme-linked immunosorbent assay; RT-qPCR, real-time quantitative polymerase chain reaction; PCoA, principal coordinate analysis; PCA, principal component analysis; LEfSe, linear discriminant analysis effect size analysis; ADH1B, alcohol dehydrogenase 1B; ALDH2, acetaldehyde dehydrogenase 2; Dx-FITC, dextran-FITC

* Corresponding authors.
E-mail addresses: liupu@lzu.edu.cn (P. Liu), xkli@lzu.edu.cn (X. Li).

https://doi.org/10.1016/j.jff.2020.104045
Received 18 December 2019; Received in revised form 19 May 2020; Accepted 30 May 2020
Available online 22 June 2020

changes the composition of gut microbiota (Engen, Green, Voigt, Forsyth, & Keshavarzian, 2015; Schnabl & Brenne, 2014), termed as gut dysbiosis, which plays a critical role in the development of alcoholic steatohepatitis (Minemura & Shimizu, 2015). For example, chronic alcohol abuse causes intestinal bacterial overgrowth, and changes the composition of gut microbiota in rodents and humans, along with systemic increases in endotoxin (lipopolysaccharide, LPS), liver steatosis and inflammation (Bull-Otterson et al., 2013; Yan & Fouts, 2011). Specific gut dysbiosis is confirmed to be correlated with alcohol-dependence severity and liver cirrhosis (Leclercq et al., 2014; Llopis et al., 2016). Additionally, the abundance of *Bacteroidetes* is significantly decreased, and that of *Actinobacteria* and *Firmicutes* are significantly increased among mice with hepatic steatosis and inflammation induced by alcohol exposure (Ferrere et al., 2017). Fecal microbiota transplantation protects alcohol-sensitive mice against ALD and recovers the gut microbiota close to that of alcohol-resistant mice, which further confirms the important role of gut microbiota in ALD (Ferrere et al., 2017). Gut microbiota is also associated with maintenance of gut integrity by protecting the intestinal barrier (Johansson, Sjövall, & Hansson, 2013). Gut dysbiosis increases intestinal permeability, which leads to gut-derived bacteria and LPS easily entering the liver (Chen, Stärkel, Turner, Ho, & Schnabl, 2015; Tuomisto et al., 2014). LPS activates nuclear factor-κB (NF-κB) pathway through Toll-like receptor (TLR) 4, resulting in liver inflammation (Hao et al., 2018). Therefore, ALD is substantially driven by gut dysbiosis, and targeting gut microbiota will be an effective therapeutic strategy for the prevention or treatment of ALD.

A variety of probiotic strains, either individually or as cocktails, are frequently used in alleviating ALD (Li, Duan, Wang, McClain, & Feng, 2016). Among these, some probiotics, like *Lactobacillus rhamnosus* R0011, *Lactobacillus acidophilus* R0052, *Lactobacillus acidophilus*, *Lactobacillus helveticus* and *Bifidobacterium*, are reported to attenuate ALD by inhibiting inflammation or endotoxemia (Hong, Kim, Han, Kim, Suk, Kim, Kim, Kim, & Baik, 2015; Marotta et al., 2005). The probiotic VLS#3 significantly decreased cytokines in alcoholic cirrhosis patients (Loguercio et al., 2005). Additionally, *Lactobacillus rhamnosus* GG supernatant and heat-killed *Lactobacillus brevis* SBC8803 also prevented alcohol-induced hepatic steatosis and inflammation in mice by improving intestinal barrier function and alleviating endotoxemia (Segawa, Wakita, Hirata, & Watari, 2008; Wang et al., 2012; Zhao et al., 2015). Recently, *Lactobacillus rhamnosus* GG prevented liver inflammation and injury through restoring microbiota diversity in mice (Bull-Otterson et al., 2013). *Bifidobacterium*, like *Bifidobacterium longum* LC67 and *Bifidobacterium bifidum*, alleviated alcohol-induced liver injury in mice and humans through restoration of the disturbed gut microbiota (Kim, Kim, Kwon, Han, & Kim, 2018; Kirpich et al., 2008). Mounting evidence suggests that restoration of gut microbiota is one of the major mechanisms underlying protective effects of probiotics on ALD. However, despite these previous reports, the relationship between modulating effects of probiotics on gut microbiota and the protective effects on ALD has not been clarified so far.

Although some *Bifidobacterium* species are reported to prevent ALD, few studies have been performed to establish their abilities in regulating immunity and enhancing intestinal barrier function. In addition, the relationship between *Bifidobacterium*, gut microbiota, and ALD in mice has remained elusive. It is well known that *Bifidobacterium breve* can promote the colonization of *Bifidobacteria*, protect immune system, strengthen the intestinal epithelium layer, and maintain intestinal homeostasis (Mortensen et al., 2019). *Bifidobacterium breve* ATCC15700 (ATCC15700), isolated from infant feces, is identified as a natural probiotic with anti-inflammatory activity (Van Beek & Hoogerland, 2015). Considering the multiple activities of *Bifidobacterium breve*, the hypothesis was that ATCC15700 may alleviate ALD by modulating immune-inflammation and intestinal barrier function through modification of gut microbiota. Therefore, the objectives of this study were to investigate the effects of ATCC15700 on chronic alcohol-induced liver injury in mice and the role of gut microbiota in mediating the effects of ATCC15700 on ALD. Our findings will provide a theoretical basis for future clinical research and the development and application of probiotics.

2. Materials and methods

2.1. Culture and preparation of ATCC15700

ATCC15700 was obtained from the American Type Culture Collection (ATCC), and cultured under anaerobic conditions at 37 °C for 12 h in BBL medium (Hangzhou Baisi Biotechnology, Hangzhou, China). ATCC15700 cultures were centrifuged at 5,000 rpm for 10 min, and washed three times with phosphate-buffered saline (PBS, pH = 7.2; NaCl 8 g/L, KCl 0.2 g/L, Na_2HO_4 1.44 g/L, KH_2PO_4 0.24 g/L). The supernatant was filtered through 0.22 μm filters until its density reached 5×10^{10} colony-forming units (CFU)/mL. ATCC15700 was re-suspended in PBS, and then stored at 0–4 °C for further use in a week.

2.2. Experimental animals and protocols

Eight-week-old adult male C57BL/6 mice (22 ± 2 g) were purchased from the Animal Center of Lanzhou University (Lanzhou, China, SCXK (GAN) 2018–0002). All mice were housed under specific pathogen-free conditions at 22 ± 1 °C and at 40–60% relative humidity for a week prior to the treatment, and were fed standard food and water freely. All animal experimental procedures were performed according to Lanzhou University's Institutional Animal Care and Use Committee guidelines (Lanzhou, China). Pure alcohol was dissolved in PBS (60% v/v). Animals were randomly divided into four groups (10 mice per group), and each mouse was maintained in a separate cage. Briefly, the PBS-treated mice (PBS group) were orally supplemented with PBS (200 μL) twice at one-hour intervals every day. The alcohol-treated mice (Alc group) were given alcohol (3.8 g/kg body weight, 200 μL) one hour after PBS administration. In ATCC15700 and alcohol-treated mice (ATCC15700 + Alc group), mice were administered with 200 μL of ATCC15700 suspension at the final dose of 10^{10} cells one hour before alcohol (3.8 g/kg body weight, 200 μL) treatment. The ATCC15700-treated mice (ATCC15700 group) were fed with ATCC15700 at the same dose with ATCC15700 + Alc group one hour before PBS administration. Alcohol and ATCC15700 suspension were orally gavaged once a day for 6 weeks.

The body weight and food intake of each mouse were measured every week. After 6 weeks of treatment, fecal samples from each mouse were collected at the end of the experiment, and then stored at −80 °C until processing. After that, gut motility and permeability assays were performed. And then, serum was collected and stored −80 °C for further investigations. All mice were killed by cervical dislocation. Tissues were removed immediately after the mice were sacrificed. The liver, ileum, and colon were collected and quickly exposed in liquid nitrogen, and stored at −80 °C until processing. Spleen tissues were harvested for flow cytometry analysis. The body and liver weight are recorded (Table S1).

2.3. Histopathology and immunohistochemistry

The liver tissues were fixed with 4% paraformaldehyde for 12 h, and then, processed to prepare 5 μm paraffin sections for hematoxylin and eosin staining (Beijing Solarbio Science & Technology, Beijing, China). Frozen tissue sections of liver were processed for staining with oil red O and then studied by light microscopy. Hepatic steatosis was analyzed semi-quantitatively and classified into five grades according to previous studies (Ferrere et al., 2017). Sections of liver, ileum, and colon, were prepared for immunohistochemical staining to determine hepatocyte proliferation and intestinal mucin-2 levels. Briefly, tissue paraffin sections (5 μm) were incubated with 3% hydrogen peroxide for 20 min and incubated at 4 °C overnight with primary antibody rabbit anti-Ki-67 or

anti-mucin-2 (Boster, Wuhan, China). Two-step immunohistochemical staining kit (Boster, Wuhan, China) was used according to the manufacturer's instructions. Sections were stained with diaminobenzidine kit (Beijing zhongshanjinqiao Biotechnology Co., Ltd., Beijing, China), and then counterstained with hematoxylin.

2.4. Biochemical analysis

Biochemical parameters were evaluated using commercial kits purchased from Nanjing Jiancheng Biology Research Institute (Nanjing, China) according to the instructions. Serum samples were prepared to determine alanine aminotransferase (ALT), aspartate aminotransferase (AST), triacylglycerol (TG), alcohol, and acetaldehyde. Liver samples were prepared by homogenization in sterile PBS, and centrifugation at 12,000 rpm for 10 min at 4 °C. The supernatant was collected and used to analyze TG, malondialdehyde (MDA), super oxide dismutase (SOD), glutathione (GSH), and catalase (CAT).

2.5. Enzyme-linked immunosorbent assay

Serum LPS was measured using mouse LPS enzyme-linked immunosorbent assay (ELISA) kits (Jianglai Biotechnology Co., Ltd., Shanghai, China) according to the manufacturer's protocols. 0.2 g liver tissue of each mouse was weighed and homogenized with PBS, and then centrifuged at 12,000 rpm for 10 min at 4 °C to get supernatant. TNF-α, interleukin (IL)-1β, IL-6 and IL-17 levels in serum and liver supernatant were measured using corresponding ELISA kits (Shanghai Enzyme-linked Biotechnology, Shanghai, China) according to the instructions.

2.6. Gene expression assay

Total RNA of each mouse were extracted from the liver and colon using TRIzol Reagent (ShineGene Molecular Biotech. Inc., Shanghai, China). Real-time quantitative polymerase chain reaction (RT-qPCR) was performed using SYBR green Master Mix on instrument FTC3000 (Canada). The cycling conditions used to amplify the complementary DNA were initiated with an activation at 94 °C for 4 min, 35 cycles at 72 °C for 30 s, consisting of a 20 s denaturation at 94 °C, and a annealing temperature at 60 °C for 25 s. The sequences of the forward and reverse primers used have been listed in Table S2. All samples were run in triplicate. The relative mRNA expression of *TNF-α*, *IL-1β*, *IL-6*, *IL-17*, *claudin-1*, *occludin*, *E-cadherin*, and *ZO-1* were calculated by the $2^{-\Delta\Delta Ct}$ method. Mouse β-actin was used to normalize the transcript levels of each biomarker. Gene expression levels were presented as fold change with setting the value of the PBS group mice as 1.

2.7. Flow cytometry for assessment of Treg and Th17

Mouse spleen mononuclear cells were isolated from fresh spleen samples with mouse 1 × lymphocyte separation medium (Dakewe Biotech Co., Ltd. Shenzhen, China), and then, prepared in RPMI 1640 media (Shanghai BasalMedia Technologies Co., LTD. Shanghai, China). Cells were stained with rat anti-mouse CD4 Alexa Fluor 647 and CD25 BB515, and incubated at room temperature in the dark for 30 min. For intracellular staining, after incubation with fixing and permeabilization reagent, cells were stained with rat anti-mouse Foxp3 PE. For detection of intracellular T helper (Th17) cells, cells were stimulated with 4 μL Leukocyte Activation Cocktail with GolgiPlug (Becton, Dickinson and Company) for 5 h, and then incubated with rat anti-mouse CD4 Alexa Fluor 647 and stained with rat anti-mouse IL-17A PE. After wash with PBS, the stained cells were acquired on an Amnis FlowSight System (Merck, USA). All fluorescent conjugated antibodies were purchased from BD (Becton, Dickinson and Company) according to the manufacturer's instructions. T regulatory (Treg) cells and Th17 cells were defined as co-expressing $CD4^+CD25^+Foxp3^+$ and $CD4^+IL\text{-}17A^+$, respectively. The data were analyzed in IDEAS software (Version 6.2).

2.8. Western blot analysis

Total proteins extraction from the liver and ileum of each mouse were performed using radio immunoprecipitation assay buffer (50 mmol Tris, pH 7.4, 150 mmol NaCl, 1% Nonidet P-40, 0.5% sodium deoxycholate, and 1 mmol/L PMSF) and centrifuged at 12,000 rpm for 20 min. The supernatant was collected and protein concentrations were determined by bicinchoninic acid kit. 20 μg proteins were loaded onto 5–12% SDS-PAGE gels. After electrophoresis, protein bands were transferred to 0.45 μm nitrocellular membranes. The membranes were blocked in 5% BSA-TBST for 60 min at room temperature, and then probed with rabbit antibody against claudin-1 (Boster, Wuhan, China), occludin (Boster, Wuhan, China), E-cadherin (Boster, Wuhan, China), ZO-1 (Boster, Wuhan, China), CYP2E1 and acetadehyde dehydrogenase 2 (ALDH2) (Proteintech Group, Inc., Chicago, USA), TLR 4 and TLR5 (Proteintech Group, Inc., Chicago, USA), and mouse antibody NF-κB P65 (Erwantech, Shanghai, China), Alcohol dehydrogenase 1B (ADH1B) (Proteintech Group, Inc., Chicago, USA) overnight at 4 °C, respectively. The membranes were washed with TBST buffer and processed with secondary antibody horseradish peroxidase-labelled goat anti-rabbit IgG. After washing with TBST buffer, the membranes were treated with enhanced chemiluminescence (Millipore, USA) western blotting reagent. Rabbit anti-β-actin antibody (Boster, Wuhan, China) was used as internal inference. At last, the density of each protein band was scanned and quantified using Image-Pro Plus 6.0.

2.9. Intestinal permeability assay

Intestinal permeability was examined using 4000 Da fluorescent-dextran-FITC (Dx-FITC; Sigma-Aldrich, USA). According to our previous study (Tian et al., 2019), after 5 h fasting, mice were orally gavaged with Dx-FITC (100 mg/mL, 200 μL). After 4 h, 200 μL blood of each mouse was collected and centrifuged at 4 °C at 5,000 rpm for 10 min. The serum was collected and stored –80 °C until use. Intestinal permeability was determined by measuring the amount of Dx-FITC in the serum with a fluorescence spectrophotometer (excitation 485 nm and emission 535 nm).

2.10. Sequencing of fecal bacterial 16S rRNA and analysis

The composition of gut microbiota was sequenced using Illumina Miseq technology (Nuozhou Biotech Co., Chengdu, China) targeting the V4-V5 region of the 16S rRNA gene. The fecal genomic DNA extraction was performed with the DNA extraction kit (Tiangen Biotech, Shanghai, China), and its quantification was carried out using Nanodrop 2000 (Thermo Fisher Scientific, USA). PCR was performed using the primer pair, 515F-909R (forward: 5′-GTGCCAGCMGCCGCGGTAA-3′; reverse: 5′-CCCCGYCAATTCMTTTRAGT-3′) with unique barcode for each sample. The PCR amplification was carried out with an initial denaturation at 94 °C for 3 min, followed by 30 cycles of 94 °C for 40 s, 56 °C for 60 s, and 72 °C for 60 s, and a final extension at 72 °C for 10 min. Two PCR reactions were conducted and then combined after amplification. The raw data were processed using QIIME Pipeline-Version 1.9.0 (http://qiime.org/scripts/split_libraries_fastq.html), and the length of sequences less than 150 bp were removed. All the sequences were clustered into operational taxonomic units (OTUs) at a 97% identity threshold. Singleton sequences were filtered out. Each sample was rarefied at 24,980 sequences for further analysis. Ribosomal Database Project (RDP) classifier was performed for taxonomy of each OTU from genus to kingdom. Alpha-diversity was generated based on observed species described as Shannon index. Principal coordinate analysis (PCoA) was conducted for the comparison of microbial community in each sample using R software (Version 3.1.0). Linear discriminant analysis (LDA) effect size analysis (LEfSe) was used to reveal the most differentially abundant taxa over-represented in gut microbiota.

Gut microbiota sequencing data reported in this study have been submitted to NCBI database and the accession number is PRJNA592297.

2.11. Statistical analysis

All data are indicated as the mean ± S.E.M. The statistical analyses between groups were performed by one-way analysis of variance (ANOVA) using GraphPad Prism Version 8.2.1 (GraphPad Software, USA), and comparisons between two groups were analyzed using Student's *t*-test. $P < 0.05$ indicates statistical significance. Principal Component Analysis (PCA) was performed, in order to study the scattering of liver injury, and PCoA was performed for the comparison of microbial community in individuals using R software (Version 3.1.0). LEfSe was used to show the statistical significance of the differentially abundant taxa represented in cladograms on the basis of LDA score > 2.

3. Results

3.1. ATCC15700 pretreatment prevents alcohol-induced liver injury in mice

To examine whether ATCC15700 pretreatment could prevent alcohol-induced liver injury, 40 male adult mice were divided randomly into four experimental groups (n = 10 per group), the control group (PBS-treated mice), the Alc group (60% alcohol, 200 μL), the ATCC15700 + Alc group (5×10^{10} CFU/mL ATCC15700 and 60% alcohol, 200 μL, respectively), the ATCC15700 group (5×10^{10} CFU/mL ATCC15700, 200 μL). All groups of mice were orally gavaged daily for 6 weeks. After 6 weeks of treatment, ATCC15700 prevented alcohol-induced decrease in body weight gain from week 2 onward (Table S1 and Fig. S1A), which was not related to the food intake of mice in four groups (Fig. S1B). Alcohol exposure significantly increased liver weight index, serum TG levels ($P < 0.0001$), and serum ALT ($P < 0.0001$) and AST ($P = 0.0002$) activities, all of which were normalized by ATCC15700 (Fig. S1C–E). Moreover, ATCC15700 attenuated alcohol-induced hepatic steatosis and hepatocyte proliferation, as shown in histological liver sections (Fig. 1A), and as indicated by significantly lower TG accumulation in the liver of ATCC15700 + Alc group mice compared to that of the Alc group ($P = 0.0063$, Fig. 1B).

In addition, ATCC15700 pretreatment significantly attenuated alcohol-induced hepatic oxidative stress by decreasing MDA ($P = 0.0002$) and increasing SOD ($P = 0.0021$), CAT ($P = 0.01$) and GSH ($P = 0.0001$) concentration in the liver (Fig. S2A–D). ATCC15700 also eliminated alcohol-induced inflammation, as indicated by the significant reduction of inflammatory cytokines (including TNF-α, IL-1β, IL-6 and IL-17) in both serum and liver (Fig. S2E–L). In line with this, ATCC15700 markedly reduced the gene expressions of *IL-1β* ($P = 0.0027$), *IL-6* ($P = 0.0008$) and *IL-17* ($P < 0.0001$) and eliminated that of *TNF-α* ($P < 0.0001$) in alcohol-exposed mice (Fig. 1C). Most specifically, the expressions of these genes in ATCC15700 group mice were obviously lower than those in the PBS group ($P < 0.0001$, respectively), suggesting ATCC15700 with anti-inflammatory properties.

Overall, based on liver injury parameters, including hepatic steatosis indicators, biochemical indices, oxidative stress and inflammation, PCA was performed. The PCA analysis showed that alcohol affected Alc group mice clearly separated from other groups along PC1 (68.7%), while ATCC15700 treatment shifted the ATCC15700 + Alc group towards the PBS group (Fig. 1D). This indicates that ATCC15700 protects alcohol-exposed mice against liver injury.

3.2. ATCC15700 alleviates endotoxemia and improves immune homeostasis in alcohol-exposed mice

Alcohol-induced liver inflammation has been reported to relate to TLR4-NF-κB pathway activated by LPS (Hao et al., 2018). Our study observed that alcohol exposure significantly increased serum LPS concentration (by 76.81%, $P = 0.003$), which was normalized by ATCC15700 supplementation (Fig. 2A). Moreover, Western blotting results showed a significant increase in the protein levels of NF-κB p65, TLR4 and TLR5 in the liver tissue of alcohol-exposed mice ($P < 0.0001$, $P = 0.0004$, and $P = 0.0007$, respectively) compared to the PBS group. In contrast, ATCC15700 administration normalized the hepatic concentration of TLR4 and NF-κB p65 and significantly reduced TLR5 ($P < 0.0001$) (Fig. 2B, C). Therefore, ATCC15700 effectively prevents liver inflammation via TLR4-NF-κB pathway-mediated pro-inflammatory response in alcohol-exposed mice.

The imbalance of Treg/Th17 cell proportion plays an important role in the pathogenesis of ALD. Therefore, we investigated whether the protective effects of ATCC15700 against ALD were associated with Treg/Th17 cell proportion. Treg and Th17 cells were represented with $CD4^+CD25^+Foxp3^+$ and $CD4^+IL\text{-}17A^+$, respectively. After 6 weeks of treatment, alcohol exposure induced a significant increase in Th17 cells ($P < 0.0001$) and a reduction in Treg cells ($P = 0.0004$), and obviously reduced Treg/Th17 cell ratios ($P = 0.0003$) in the spleen (Fig. 2D–H), which were restored by ATCC15700 administration. Collectively, these data suggest that ATCC15700 could alleviate endotoxemia and LPS-mediated liver inflammation, and maintain immune homeostasis.

3.3. ATCC15700 pretreatment improves intestinal barrier function in alcohol-exposed mice

To explore potential mechanisms how ATCC15700 prevented ALD, we firstly assessed the effects of ATCC15700 pretreatment on alcohol metabolism. ATCC15700 did not metabolize alcohol *in vitro* and had no significant effect on serum alcohol concentrations in alcohol-exposed mice (Fig. S3A, B). Although ATCC15700 administration partly decreased serum acetaldehyde levels ($P = 0.0475$) (Fig. S3C) and induced a significant increase in hepatic ADH1B ($P = 0.0011$) and ALDH2 ($P = 0.0026$) protein levels and a reduction in CYP2E1 levels ($P = 0.0008$) in alcohol feeding mice (Fig. S3D, E), there are still rather high levels of alcohol and acetaldehyde in the serum. Therefore, we excluded the possibility that ATCC15700 does not seem to metabolize alcohol in a significant extent. There, however, may be a minor effect on generation of toxic acetaldehyde. Furthermore, ATCC15700 had the ability to resist alcohol and acid *in vitro*, and could colonize in the intestinal tracts of mice (Fig. S3F–H). Therefore, we speculate that ATCC15700 may have impact on the intestinal microbiota.

Immunohistochemistry analysis revealed alcohol consumption remarkably decreased the expression of mucin-2 in both ileum ($P = 0.0008$) and colon ($P = 0.0044$) compared to PBS group mice, which were reversed after ATCC15700 administration (Fig. 3A–C), indicating that ATCC15700 enhances mucin-2 production. Moreover, alcohol exposure caused a significant reduction in tight junction protein claudin-1, occludin, E-cadherin, and ZO-1 in the ileum ($P = 0.0005$, $P = 0.0018$, $P = 0.0051$, and $P = 0.0101$, respectively), which were normalized by ATCC15700 pretreatment (Fig. 3D, E). ATCC15700 also significantly reversed the expressions of *occludin* ($P = 0.012$), *E-cadherin* ($P = 0.0073$) and *ZO-1* ($P = 0.0115$) in the colon of alcohol-treated mice (Fig. 3F). Interestingly, gene expressions of *occludin*, *E-cadherin* and *ZO-1* were obviously higher in ATCC15700 group mice than those in the PBS group ($P = 0.0015$, $P < 0.0001$, and $P = 0.0059$; respectively), suggesting that ATCC15700 increases the expressions of tight junction proteins in the intestine. To further investigate whether mucin-2 or tight junction proteins impact on intestinal barrier integrity, intestinal permeability was examined by measuring serum Dx-FITC levels. Compared to PBS group mice, alcohol exposure significantly increased serum Dx-FITC levels (394.21 ± 23.45 versus 202.79 ± 17.04 ng/mL, $P < 0.0001$), which was normalized by ATCC15700 administration (Fig. 3G), suggesting that ATCC15700 prevents alcohol-induced intestinal hyper-

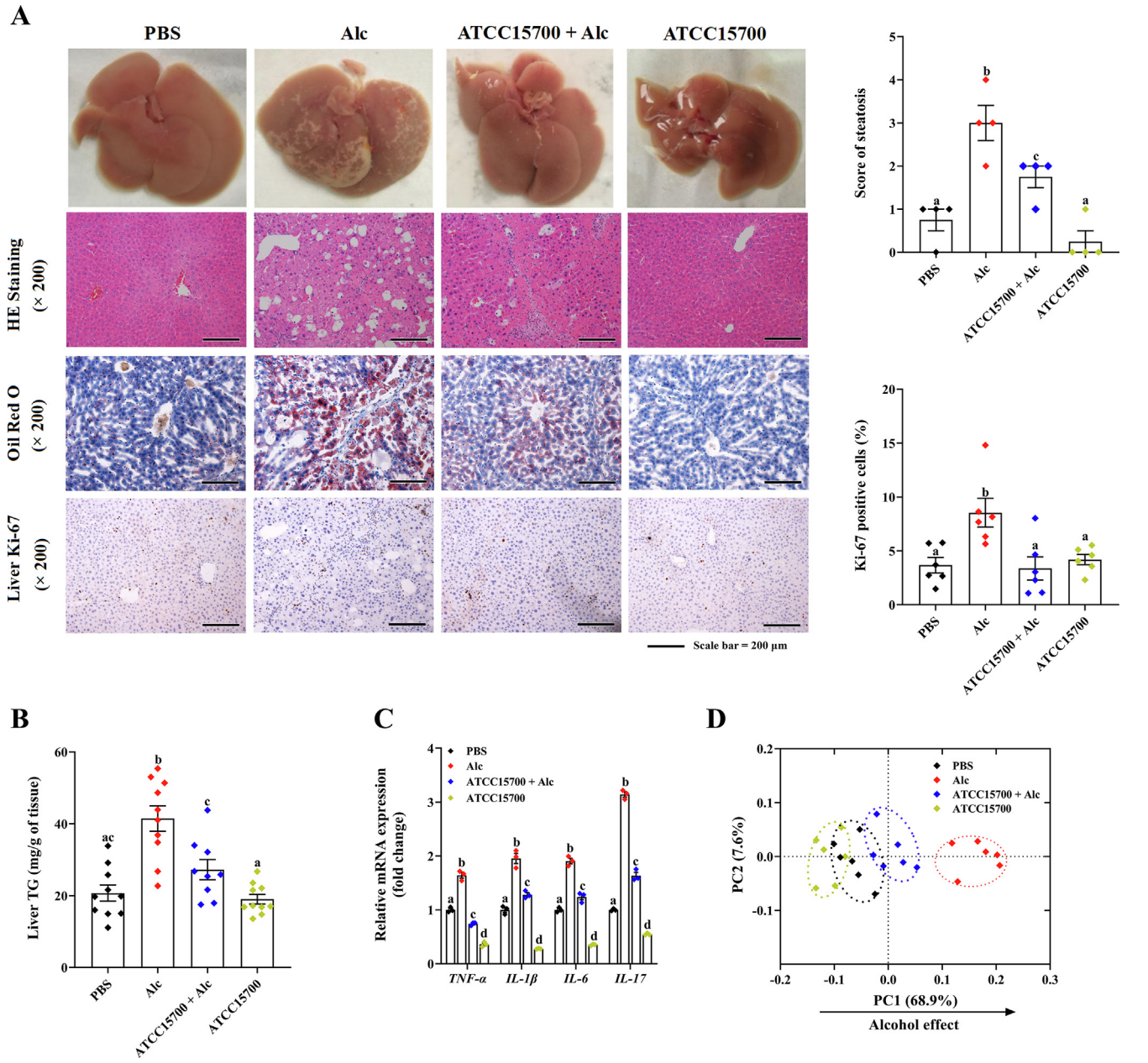

Fig. 1. ATCC15700 pretreatment prevents alcohol-induced liver injury in mice. (A) Liver picture and the representative photomicrographs of HE, oil red O and immunohistochemical staining liver sections. The scale bar = 200 μm. (B) Liver TG. (C) Relative gene expression of *TNF-α*, *IL-1β*, *IL-6* and *IL-17* in the liver. (D) PCA for liver injury parameters of four group mice. The data are expressed as mean ± S.E.M. (n = 3–10). Bars with different letters represent significant differences between groups by student's *t*-test ($P < 0.05$).

permeability. Taken together, these data indicate that ATCC15700 improves intestinal barrier function by enhancing the expression of tight junction proteins. Furthermore, ATCC15700 promoted the intestinal motility in alcohol-exposed mice via decreasing total transit time and increasing defecation rate (Fig. S4). Endotoxemia, intestinal permeability and motility are associated with gut microbiota (Yano et al., 2015). Therefore, the protective effects of ATCC15700 against ALD may be originating from modulation of gut microbiota.

3.4. Effects of ATCC15700 pretreatment on the structure and composition of gut microbiota in alcohol-exposed mice

It is well known that gut dysbiosis is a major contributor to the development of ALD (Ferrere et al., 2017). Here, we analyzed and compared the bacterial composition and diversity of fecal samples from all mice at the end of experiments using Miseq sequencing. The alpha-diversity, assessed by Shannon index and observed species, showed that bacterial diversity of Alc group mice was significantly higher than that of the PBS group ($P = 0.001$ and $P = 0.009$, respectively), which was restored after ATCC15700 treatment (Fig. 4A, B). Beta-diversity analysis based on PCoA analysis revealed that phylogenetic community structures were significantly different between Alc group samples and other groups, and the Alc group was clearly separated from others along PCoA1 (22.05%). However, ATCC15700 obviously shifted the overall structure of the alcohol-disturbed gut microbiota towards that of the PBS group (Fig. 4C). At the phylum level, *Bacteroidetes*, *Firmicutes*, *Proteobacteria*, *Tenericutes*, *Deferribacteres*, *Verrucomicrobia*, and *Cyanobacteria* were the dominant phylum in the feces of all groups of mice (relative abundance > 0.5%, Fig. 4D, E). Compared with PBS group mice, the relative abundance of *Bacteroidetes* (52.14 ± 2.35% versus

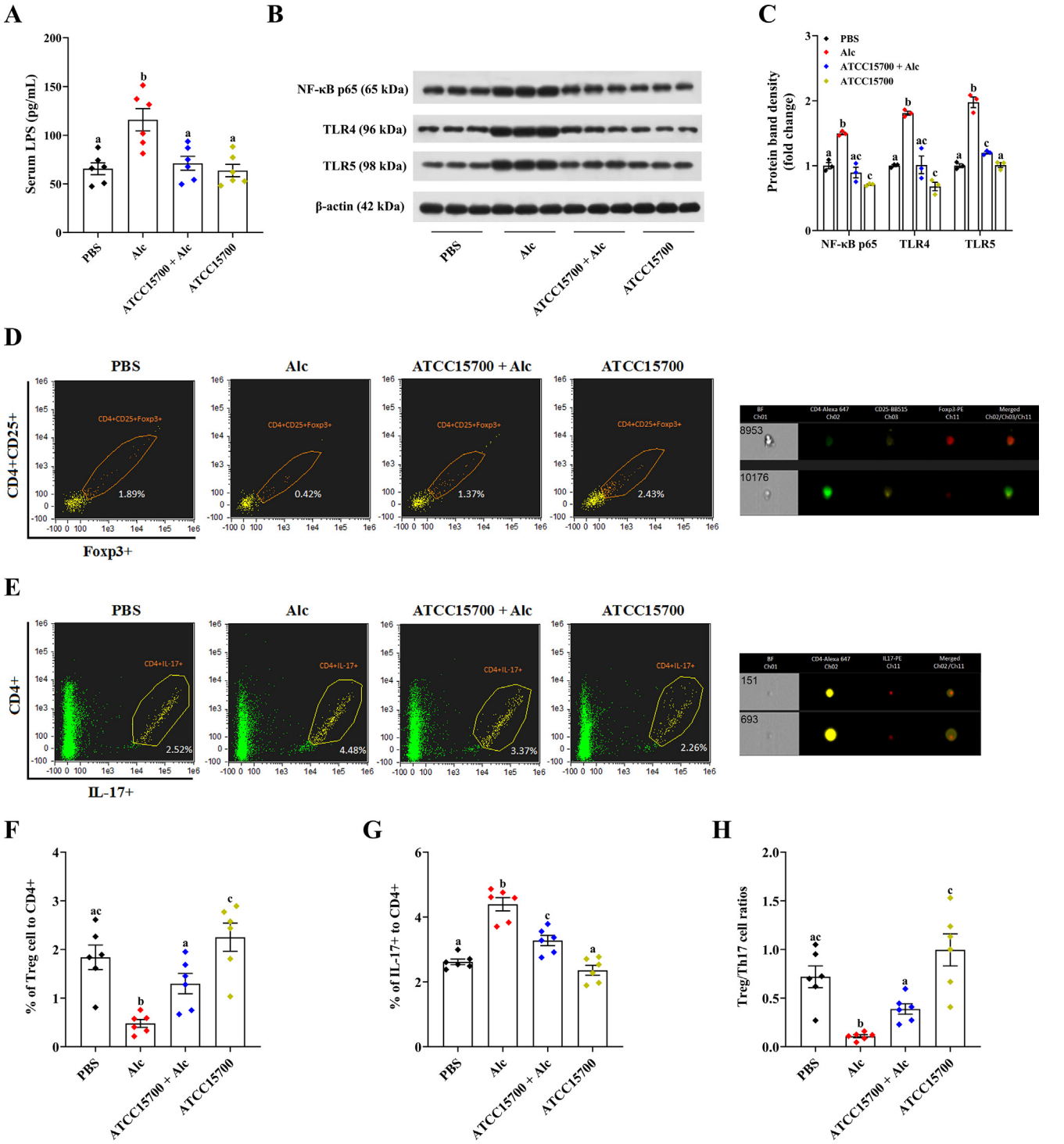

Fig. 2. ATCC15700 pretreatment alleviates endotoxemia and TLR4-NF-κB pathway-mediated pro-inflammatory response, and maintains immune homeostasis in alcohol-exposed mice. (A) Serum LPS levels. (B) Western blotting of hepatic NF-κB, TLR4 and TLR5. (C) Quantitative analysis of hepatic protein concentrations. (D) Representative flow cytometric plots of $CD4^+CD25^+Foxp3^+$ Treg cells labeled with the corresponding percentage of $CD4^+$ T cells on the basis of representative images of treated cells, for improved visualization, green (Alexa 647), yellow (BB515), and red (PE) colors were assigned in IDEAS software 6.2. (E) Representative flow cytometric plots of $CD4^+IL\text{-}17A^+$ TH17 cells labeled with the corresponding percentage of $CD4^+$ T cells on the basis of representative images of treated cells, for improved visualization, yellow (Alexa 647) and red (PE) colors were assigned in IDEAS software 6.2. (F) The percentage of Treg cells to $CD4^+$ T cells. (G) The percentage of TH17 cells to $CD4^+$ T cells. (H) The ratio of Treg cells to TH17 cells. The data are expressed as mean ± S.E.M. (n = 3–10). Bars with different letters represent significant differences between groups by student's *t*-test ($P < 0.05$). (For interpretation of the references to color in this figure legend, the reader is referred to the web version of this article.)

66.46 ± 2.29%, $P = 0.0004$) significantly decreased, and that of *Firmicutes* ($P = 0.0003$) and *Deferribacteres* ($P = 0.0251$) significantly increased in the Alc group. ATCC15700 pretreatment restrained alcohol-induced decrease in *Bacteroidetes* (Fig. 4F) and increase in *Firmicutes* and *Deferribacteres* (Fig. 4G, H). Moreover, alcohol exposure significantly increased the ratio of *Firmicutes* to *Bacteroidetes* (Firm/Bac

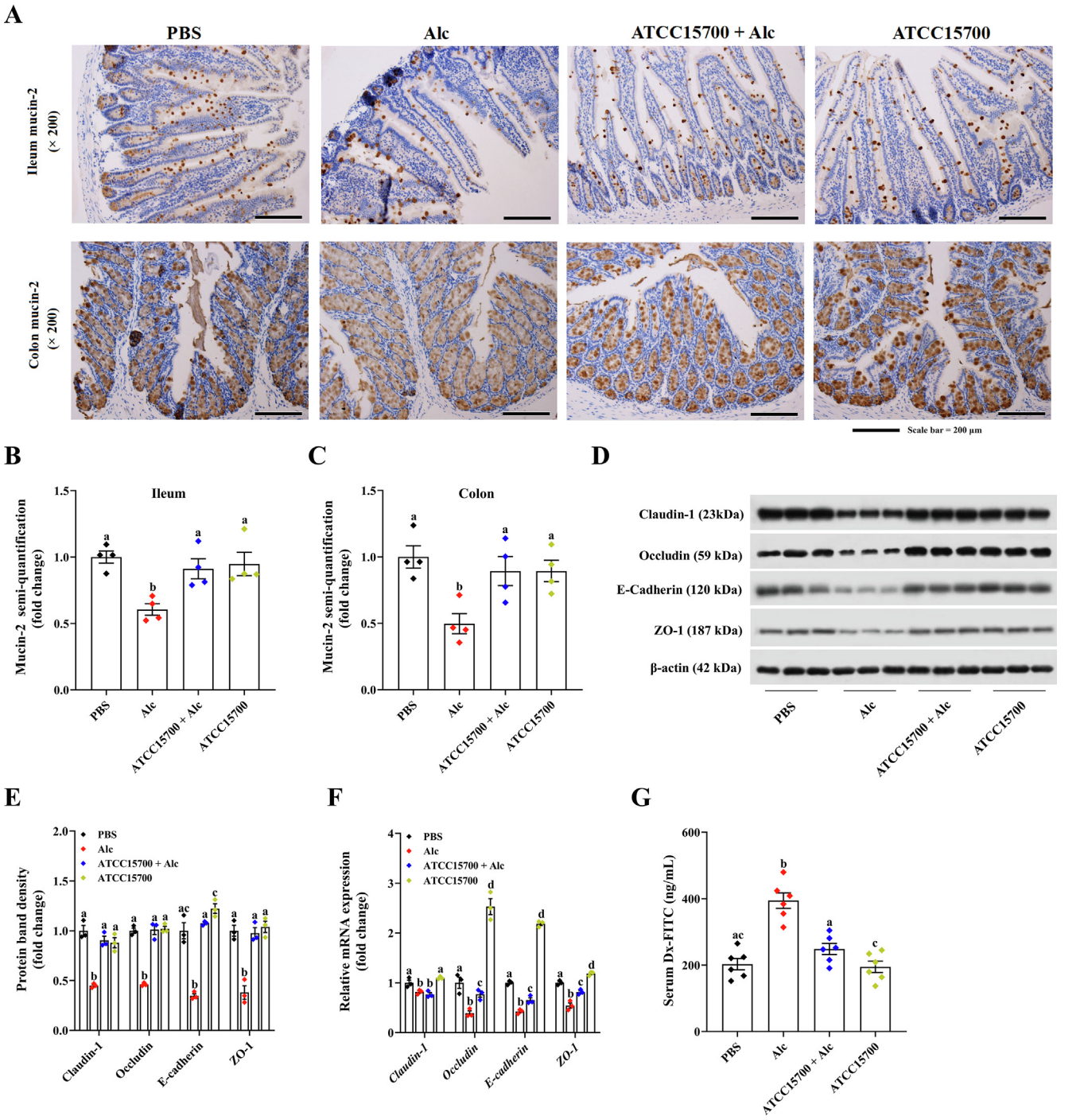

Fig. 3. ATCC15700 pretreatment improves intestinal barrier function in alcohol-exposed mice. (A) Immunohistochemical staining with mucin-2 in the ileum and colon sections. (B) Musin-2 semi-quantification in the ileum. (C) Musin-2 semi-quantification in the colon. (D) Western blotting of tight junction proteins in the ileum. (E) Protein band density quantitative analysis. (F) Relative gene expression of tight junction proteins in the colon. (G) Serum Dx-FITC. The data are expressed as mean ± S.E.M. (n = 3–6). Bars with different letters represent significant differences between groups by student's *t*-test ($P < 0.05$).

ratio) ($P = 0.0003$) compared to the PBS group, and normalized by ATCC15700 (Fig. 4I). Additionally, at the genus level, the relative abundance of *Prevotella* ($P = 0.0291$) and *S24_7* ($P = 0.0391$) significantly decreased after alcohol exposure, while that of unclassified *Clostridiales* ($P = 0.0205$), *Oscillospira* ($P < 0.0001$), *Odoribacter* ($P = 0.025$), *Mucispirillum* ($P = 0.0251$), *Butyricicoccus* ($P = 0.004$), *Ruminococcus* ($P = 0.0034$), unclassified *Desulfovibrionaceae* ($P < 0.0001$) and unclassified *Lachnospiraceae* ($P = 0.0278$) significantly increased, most of which (except *Prevotella*, *Odoribacter* and unclassified *Desulfovibrionaceae*) were restored by ATCC15700 pretreatment (Fig. S5).

Furthermore, to analyze most differentially abundant taxa in gut microbiota from phylum to genus and their phylogenic relationship, we performed LEfSe analyses and corresponding LDA scores to generate the cladograms (Fig. 5A–D). *Butyricicoccus*, *Oscillospira* and *Ruminococcus* of the *Ruminococcaceae* family, unclassified *Lachnospiraceae* of the *Clostridiales* order, *Desulfovibrio* of the *Desulfovibrionaceae* family, *Mucispirillum* of the *Deferribacteraceae* family, and *F16* of the *TM7* phylum were enriched in Alc group mice, while *Helicobacteraceae* of the *Campylobacterales* order as well as *S24_7* of the *Bacteroidales* order were under-

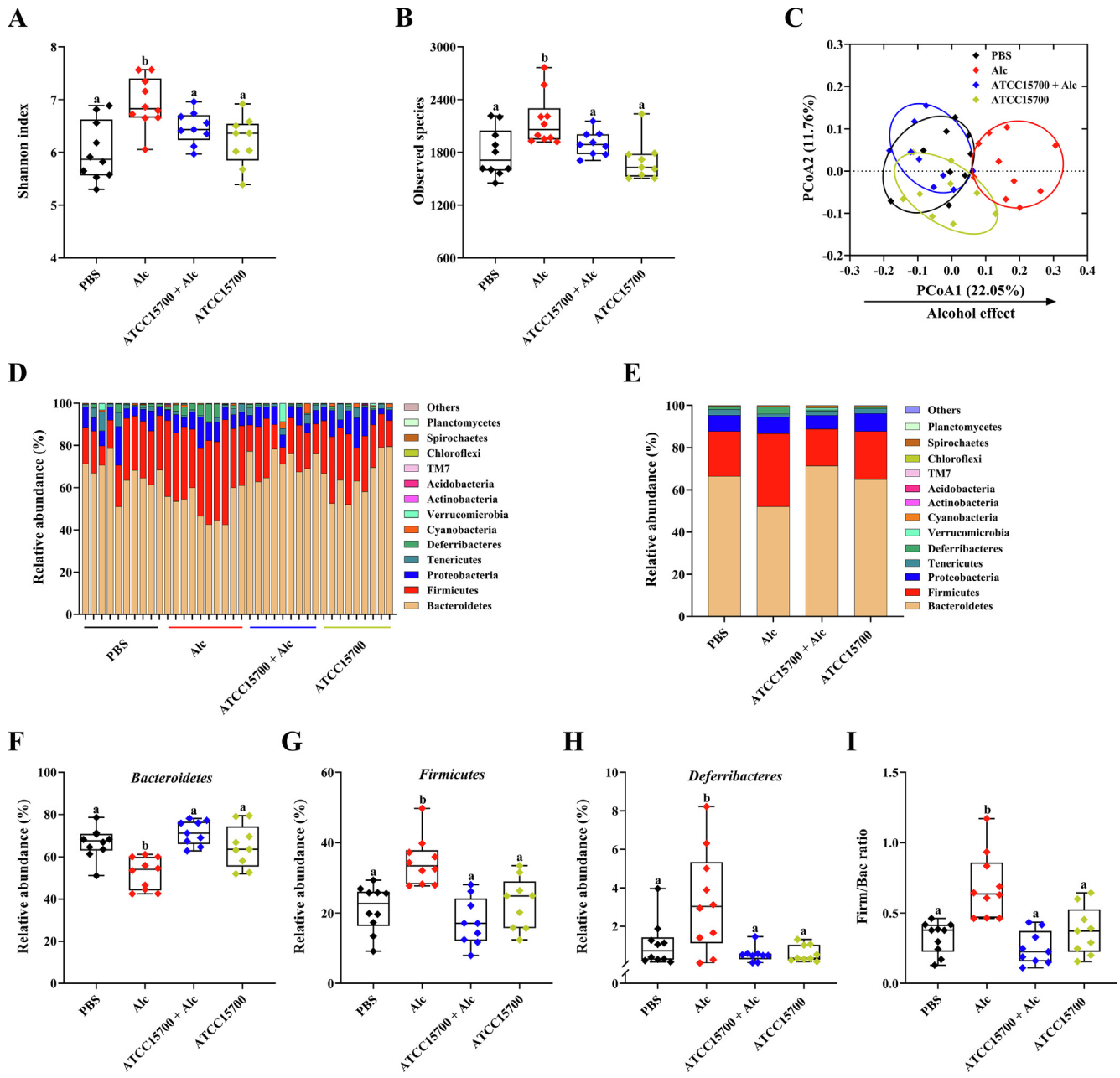

Fig. 4. Effects of ATCC15700 pretreatment on the structure and composition of gut microbiota in alcohol-exposed mice. (A) Shannon index. (B) Observed species. (C) PCoA. (D) Relative abundance of each fecal microbial profile at the phylum level. (E) Relative abundance of phyla in the gut microbiota of four groups. Relative abundance of *Bacteroidetes* (F), *Firmicutes* (G), and *Deferribacteres* (H). (I) Ratios of Firm/Bac. The data are expressed as mean ± S.E.M. (n = 9–10). Bars with different letters represent significant differences between groups by student's *t*-test ($P < 0.05$).

represented. ATCC15700 pretreatment mostly prevented the changes in taxa composition induced by alcohol exposure (Fig. 5A–C and Fig. S6A–C). Additionally, the abundances of *Helicobacteraceae* and *Desulfovibrionaceae* in the ATCC15700 + Alc group mice were obviously different from the PBS group (Figs. 5D and S6D), suggesting that their functions appear to be considerably smaller. The abundances of *Desulfovibrio* and *F16* in the gut microbiota of each sample were too low to participate in the regulation of physiological function. Therefore, *S24_7*, *Butyricicoccus*, *Oscillospira*, *Ruminococcus*, *Mucispirillum* and unclassified *Lachnospiraceae* may be more sensitive to alcohol and mainly involved in the development of ALD.

3.5. Correlation between gut microbiota and ALD

To determine the relationship between gut microbiota and ALD, Spearman's correlation analysis was performed. We firstly assessed associations between liver injury parameters and overall microbiota structure based on PCoA coordinates. Structural changes in the gut microbiota along PCoA1 were significantly associated with hepatic steatosis, inflammation, and oxidative stress (Table S3), suggesting that alcohol-induced gut dysbiosis plays a pivotal role in the pathogenesis of ALD. In addition, there are 16 key gut microbial taxa that occupy more than 90% of each sample. The correlation analysis between these bacteria and liver damage parameters was shown in Fig. 6. Among these, *Butyricicoccus*, *Oscillospira*, *Ruminococcus*, *Mucispirillum*, *Odoribacter*, unclassified *Desulfovibrionaceae* and unclassified *Lachnospiraceae* were

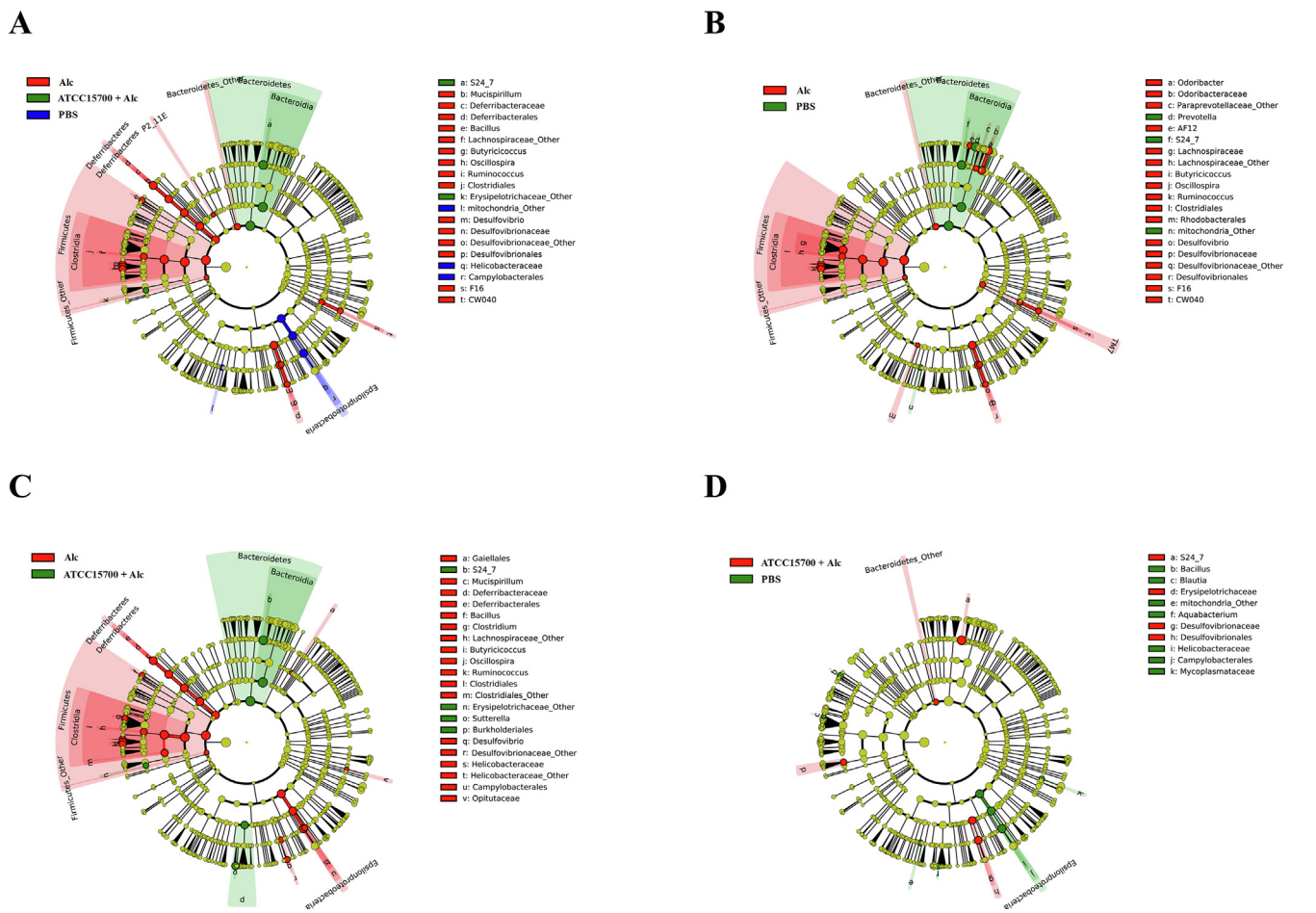

Fig. 5. Cladogram generated from LEfSe shows the most differentially abundant taxa in gut microbiota from phylum to genus. Circle's diameter is proportional to bacterial relative abundance. Differences are represented in the color for the most abundant. (A) Alc group (red), ATCC15700 + Alc group (green) and PBS group (blue). (B) Alc group (red) and PBS group (green). (C) Alc group (red) and ATCC15700 + Alc group (green). (D) ATCC15700 + Alc group (red) and PBS group (green). (For interpretation of the references to color in this figure legend, the reader is referred to the web version of this article.)

positively correlated with hepatic steatosis (liver weight index, score of hepatic steatosis and liver TG), while *Bacteroides*, *Lactobacillus* and *Prevotella* were negatively correlated with hepatic steatosis. Furthermore, *S24_7* and *Bacteroides* showed marked negative correlations with hepatocyte proliferation whereas unclassified *Clostridiales*, *Mucispirillum*, *Ruminococcus* and unclassified *Desulfovibrionaceae* showed significant positive correlations.

We further analyzed the correlations between these key bacteria and indicators of liver inflammation (serum LPS and liver inflammatory cytokines). Serum LPS was negatively correlated with *Prevotella* and positively correlated with unclassified *Clostridiales*, *Mucispirillum*, and *Ruminococcus*. Inflammatory cytokines, including TNF-α, IL-6 and IL-17, were negatively correlated with *Lactobacillus*. *Butyricicoccus*, unclassified *Desulfovibrionaceae*, and *Mucispirillum* showed significant positive correlations with TNF-α, IL-β, and IL-6. *Odoribacter* showed significant positive correlation with TNF-α, IL-β, and IL-17. We also evaluated the relationship between gut microbiota and oxidative stress parameters. *Butyricicoccus*, unclassified *Desulfovibrionaceae*, *Mucispirillum*, and *Odoribacter* were positively correlated with MDA, and *S24_7* was positively correlated with liver SOD. Unclassified *Clostridiales*, *Butyricicoccus*, *Oscillospira*, *Ruminococcus*, *Mucispirillum*, *Odoribacter* and unclassified *Desulfovibrionaceae* showed negative correlations with at least one antioxidant enzyme (SOD, GSH or CAT). In addition, correlation analysis between gut microbiota and serum Dx-FITC revealed that unclassified *Clostridiales*, *Butyricicoccus*, *Oscillospira*, *Ruminococcus*, *Mucispirillum* and *Odoribacter* as well as unclassified *Desulfovibrionaceae* were positively correlated with intestinal permeability (Fig. S7). ATCC15700 pretreatment restored the abundance of some of these key bacteria in alcohol-exposed mice, including *S24_7*, unclassified *Clostridiales*, *Butyricicoccus*, *Oscillospira*, *Ruminococcus*, *Mucispirillum* and unclassified *Lachnospiraceae*. These data indicate that these specific bacteria may be major contributors to ALD and involved in the protective effects of ATCC15700 against ALD in alcohol-exposed mice.

4. Discussion

The available evidence suggests that probiotics are capable of modulating gut microbiota and protecting intestinal mucosal integrity to decrease the oxidative stress and inflammatory response, endotoxemia, and intestinal permeability in ALD (Li et al., 2016). Recently, several studies have identified that alcohol consumption disturbs the structure and composition of gut microbiota and gut dysbiosis is significantly associated with ALD (Ferrere et al., 2017; Llopis et al., 2016). Certain probiotic strains, such as *Lactobacillus rhamnosus* GG, *Lactobacillus rhamnosus* CCFM1107, *Lactobacillus plantarum* 8PA3, *Lactobacillus plantarum* LC27, *Bifidobacterium longum* LC67, and *Bifidobacterium bifidum* attenuate ALD by modulating gut microbiota (Bull-Otterson et al., 2013; Kim et al., 2018; Kirpich et al., 2008; Tian et al., 2015). However, the relationship between modulating effects of probiotic on gut microbiota and its protective effects on ALD has not yet been well studied. In the present study, we demonstrated that ATCC15700 pretreatment prevented ALD in mice by enhancing immune response, inhibiting inflammation, and improving intestinal

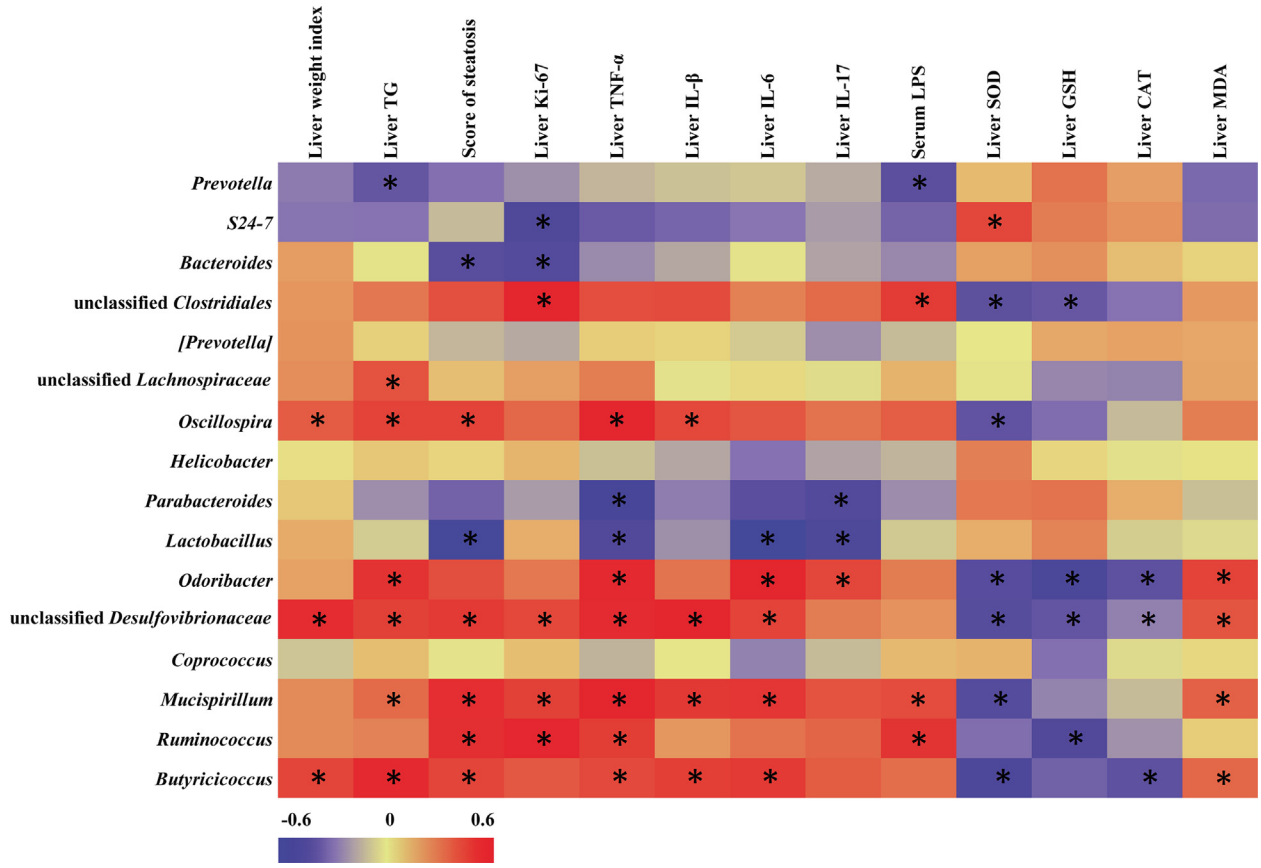

Fig. 6. Heat map shows the correlations between gut microbiota and liver damage parameters (including hepatic steatosis indicators, inflammation and oxidative stress). Significant difference is represented by asterisk.

barrier function through restoration of alcohol-disturbed gut microbiota. Importantly, we found that specific bacteria in the gut microbiota are sensitive to alcohol and significantly associated with the development of ALD.

It has been demonstrated that probiotics prevent alcohol-induced liver enlargement and lipid accumulation, and attenuate hepatic steatosis (Lu et al., 2018). *Lactobacillus plantarum* LC27 and *Bifidobacterium longum* LC67 mitigate alcoholic steatosis, along with decreasing the activities of ALT and AST in serum and TG levels in the liver (Kim et al., 2018). Similarly, we observed that ATCC15700 pretreatment significantly reduced the increases of serum ALT and AST as well as accretion of fat granules in the liver in alcohol-exposed mice. Moreover, ATCC15700 pretreatment prevented alcohol-induced liver inflammation and oxidative stress, which is in line with previous study that *Lactobacillus rhamnosus* GG and *Bifidobacterium animalis* subsp. *lactis* KV9 attenuate alcohol-induced hepatic inflammation and liver injury in mice via inhibition of TLR4-mediated endotoxin activation (Wang et al., 2013; Zhang et al., 2019).

Accumulating evidence has demonstrated that LPS-induced endotoxemia plays an important role in humans and animal models with ALD (Bode, Kugler, & Bode, 1987; Mathurin et al., 2000). Alcohol exposure increases serum LPS and hepatic TLR4 protein levels, and activates TLR4-NF-κB pathway, resulting in pro-inflammatory response and liver injury (Hao et al., 2018). A cocktail of probiotics, including *Lactobacillus acidophilus*, *Lactobacillus helveticus*, and *Bifidobacterium*, protects against ALD and endotoxemia in rat (Marotta et al., 2005). *Lactobacillus rhamnosus* R0011 and *Lactobacillus acidophilus* R0052 decrease alcohol-induced systemic and intestinal TNF-α and IL-1β levels by inhibiting the expression of TLR4 in mice (Hong et al., 2015). In accordance with our study, we found that ATCC15700 pretreatment significantly alleviated endotoxemia and TLR4-NF-κB pathway-mediated pro-inflammatory response in alcohol-exposed mice. Importantly, ATCC15700 alone treatment in ATCC15700 group mice significantly decreased the expressions of *TNF-α*, *IL-1β*, *IL-6* and *IL-17* in the liver compared to the PBS group. This indicates that ATCC15700 has anti-inflammatory properties. Furthermore, LPS is reported to stimulate Th17 cells proliferation and promote the production of IL-17 and autoimmune inflammation via activating TLR4 signaling pathway (Reynolds, Martinez, Chung, & Dong, 2012). We found that ACC15700 could balance the proportion of Treg/Th17 in the spleen in alcohol-exposed mice, which is similar to previous finding that *Lactobacillus rhamnosus* GG reversed alcohol-disturbed populations of Treg and Th17 cells (Chen et al., 2016). Taken together, these data indicate that ATCC15700 could prevent liver inflammation and maintain immune homeostasis probably through its anti-inflammatory properties. However, ATCC15700 did not metabolize alcohol *in vitro* and *in vivo*. Alcohol and acetaldehyde directly disrupt intestinal epithelial integrity and impair hepatic proteins and DNA (Leung & Nieto, 2013). Therefore, and based on alteration of intestinal microbiota and its function, intestinal barrier function may be involved in the protective effects of ATCC15700 against ALD.

LPS-mediated liver inflammation is associated with leaky gut via the gut-liver axis, and disruption of the intestinal barrier results in ALD (Chen et al., 2015). Alcohol exposure decreases the number of musin-2 positive cells in the colon, leading to the loss of mucin-2 expression in mice with ALD (Ferrere et al., 2017; Llopis et al., 2016). In our study, ATCC15700 protected mice from alcohol-induced loss of mucin-2 in the ileum and colon. In addition, chronic or acute alcohol treatment induces intestinal hyper-permeability by impairing tight junction proteins (Hao et al., 2018; Wang et al., 2012). *Lactobacillus brevis* SBC8803, *Lactobacillus rhamnosus* GG and its supernatant significantly improve intestinal tight junction proteins in mouse and human models with ALD

(Chen et al., 2016; Wang et al., 2011, 2012). The probiotic VSL#3 decreased serum endotoxin and ameliorates liver lesions via improving gut permeability in rats (Chang, Sang, Tong, Zhang, & Wang, 2013). Similarly, we found that ATCC15700 pretreatment increased the levels of tight junction proteins (including occludin, claudin-1, E-cadherin, and ZO-1) in the ileum in alcohol-exposed mice. Notably, ATCC15700 alone treatment obviously increased the expressions of *occludin*, *E-cadherin*, and *ZO-1* in the colon, suggesting that ATCC15700 could enhance the expression of tight junction proteins. Serum Dx-FITC levels further confirmed that ATCC15700 decreased alcohol-induced intestinal hyper-permeability. Taken together, our results indicate that ATCC15700 attenuates intestinal permeability and improves intestinal barrier function by increasing the expressions of intestinal tight junction proteins.

Experimental and clinical data indicate that alcohol consumption influences the composition of gut microbiota, and gut dysbiosis plays a crucial role in the pathogenesis of ALD (Cassard & Ciocan, 2018). Some studies confirmed that alcohol exposure induced gut dysbiosis, but did not significantly influence gut microbiota diversity in humans and mice with ALD (Ferrere et al., 2017; Llopis et al., 2016). Moderate and voluntary ethanol consumption increased gut microbiota alpha diversity in humans, while significantly decreased species richness in rats (Kosnicki et al., 2019). Our results indicate that alcohol exposure increased bacterial diversity and changed the structure of gut microbiota, which were normalized by ATCC15700 pretreatment. In alcoholism gut dysbiosis was associated with a decrease in the abundance of *Bacteroidetes* and an increase in that of *Enterobacteriaceae* and *Proteobacteria* (Mutlu et al., 2012). In mice alcohol intake induced a significant decrease in the abundance of *Bacteroidetes* and *Firmicutes*, and an increase in that of *Proteobacteria* and *Actinobacteria* (Bull-Otterson et al., 2013). A mixture probiotics of *Lactobacillus plantarum* LC27 and *Bifidobacterium longum* LC67 prevented alcohol-induced decrease in *Bacteroidetes* and increase in *Firmicutes*, and alleviated alcoholic steatosis by modulating gut microbiota (Kim et al., 2018). Similarly, ATCC15700 reversed alcohol-induced increases in *Firmicutes* and *Deferribacteres*, and decrease in *Bacteroidetes*. Furthermore, correlation analysis showed that the primary changes of gut microbiota along PCoA1 induced by alcohol treatment were significantly and positively correlated with hepatic steatosis, inflammation, and oxidative stress. Taken together, these results demonstrate that ATCC15700 prevents ALD via restoring gut microbiota.

In our study, 16 dominant bacteria at the genus level were found more than 90% of the gut microbiota. Among these, the abundance of *Prevotella* and *S24_7* were deceased, while that of unclassified *Clostridiales*, *Butyricicoccus*, *Ruminococcus*, *Oscillospira*, *Mucispirillum*, *Odoribacter* as well as unclassified *Lachnospiraceae* and unclassified *Desulfovibrionaceae* were increased in alcohol-exposed mice. Similarly, patients with alcohol-induced liver cirrhosis were reported to be associated with a decrease in abundance of *Prevotella* and an increase of *Ruminococcus*, *Lactobacillus*, and *Bifidobacterium* (Dubinkina et al., 2017). The abundance of *Ruminococcaceae* and *Butyricicoccus* was significantly higher in both rat and human alcohol drinkers (Kosnicki et al., 2019). On the contrary, *Lachnospiraceae*, *Ruminococcaceae*, *Lactobacillus* and *Bifidobacterium* are identified as health-associated bacteria, which are drastically reduced in alcohol dependent and liver cirrhosis patients (Chen et al., 2011; Leclercq et al., 2014). Alcohol increased the abundance of *Prevotella*, *Odoribacteriaceae* and *Clostridiaceae* and decreased that of *Clostridiales*, *Coprococcus*, *Lachnospiraceae* and *Ruminococcus* in alcohol sensitive mice with ALD (Ferrere et al., 2017). In addition, we found that alcohol-induced liver injury was negative correlated with *S24_7*, *Bacteroides*, *Lactobacillus* and *Prevotella*, and correlated positively with unclassified *Clostridiales*, *Butyricicoccus*, *Oscillospira*, *Ruminococcus*, *Mucispirillum*, *Odoribacter*, unclassified *Desulfovibrionaceae* and unclassified *Lachnospiraceae*. We also found that unclassified *Clostridiales*, *Butyricicoccus*, *Oscillospira*, *Ruminococcus*, *Mucispirillum*, *Odoribacter* and unclassified *Desulfovibrionaceae*, were positively correlated with intestinal permeability. Furthermore, ATCC15700 restored some specific bacteria in alcohol-exposed mice, including *S24_7*, unclassified *Clostridiales*, *Butyricicoccus*, *Oscillospira*, *Ruminococcus*, *Mucispirillum* and unclassified *Lachnospiraceae*. Thus, ATCC15700 alleviated alcohol-induced liver injury and intestinal barrier dysfunction most likely via the improvement of these bacteria. Overall, there are specific bacteria in the gut that are sensitive to alcohol and significantly associated with the protective effects of ATCC15700 against ALD. However, a previous study showed that alcohol-dependent subjects with high intestinal permeability have a drastically lower abundance of *Ruminococcus*, *Faecalibacterium*, *Subdoligranulum*, *Oscillibacter* and *Anaerofilum* (Leclercq et al., 2014). Reduction of *Lachnospiraceae* contributes to increased intestinal permeability and blood endotoxins, resulting in inflammation and liver injury in patients with alcohol dependence syndrome (Mutlu et al., 2012). These results are different from our study. The differences in alcohol-induced gut dysbiosis may be due to the amount of alcohol, the length of drinking or severity of liver injury. This suggests that intestinal commensal bacteria are not absolutely beneficial or harmful in the gut. Therefore, studies targeting specific bacteria are needed to elucidate their impact in the pathogenesis of ALD.

5. Conclusions

In summary, our results showed that oral administration of ATCC15700 prevented liver steatosis and inflammation, maintained immune homeostasis, improved intestinal barrier function, and modulated gut microbiota in chronic alcohol-exposed mice. Furthermore, the findings indicate that specific bacteria in gut microbiota play a role in the development of ALD and participated in the protective effects of ATCC15700. Therefore, alterations of specific bacteria or key taxa in the gut microbiota can be used to predict disease, and targeting gut microbiota mediated by probiotics may be a promising therapeutic strategy for the prevention or treatment of ALD. Our results provide a theoretical basis for future clinical research and the development and application of probiotics.

Ethical statement

All animal experimental procedures were performed in the Animal Center of Lanzhou University, and carried out in accordance with the U.K. Animals (Scientific Procedures) Act, 1986 and associated guidelines. Animal experiments were also approved by Lanzhou University's Institutional Animal Care and Use Committee guidelines.

CRediT authorship contribution statement

Xiaozhu Tian: Conceptualization, Methodology, Investigation, Software, Writing - original draft. **Rong Li:** Investigation, Writing - original draft. **Yiming Jiang:** Software, Writing - review & editing. **Fei Zhao:** Investigation, Resources. **Zhengsheng Yu:** Software, Validation. **Yiqing Wang:** Resources, Writing - review & editing. **Zixing Dong:** Resources. **Pu Liu:** Writing - review & editing, Project administration. **Xiangkai Li:** Supervision, Funding acquisition.

Declaration of Competing Interest

The authors declared that there is no conflict of interest.

Acknowledgement

The work was supported by National Natural Science Foundation Grant (No: 31870082 and 81860716), Gansu Province Major Science and Technology projects (No: 17ZD2WA017), and Gansu Province Foundation for Distinguished Young Scholars (No: 18JR3RA262).

Appendix A. Supplementary material

Supplementary data to this article can be found online at https://doi.org/10.1016/j.jff.2020.104045.

References

Basuroy, S., Sheth, P., Mansbach, C., & Rao, R. (2005). Acetaldehyde disrupts tight junctions and adherens junctions in human colonic mucosa: Protection by EGF and L-glutamine. *American Journal of Physiology-Gastrointestinal and Liver Physiology, 289*(2), G367–G375.

Bode, C., Kugler, V., & Bode, J. C. (1987). Endotoxemia in patients with alcoholic and non-alcoholic cirrhosis and in subjects with no evidence of chronic liver disease following acute alcohol excess. *Journal of Hepatology, 4*(1), 8–14.

Bull-Otterson, L., Feng, W., Kirpich, I., Wang, Y., Qin, X., Liu, Y., & Petrosino, J. (2013). Metagenomic analyses of alcohol induced pathogenic alterations in the intestinal microbiome and the effect of Lactobacillus rhamnosus GG treatment. *PloS One, 8*(1), e53028.

Cassard, A. M., & Ciocan, D. (2018). Microbiota, a key player in alcoholic liver disease. *Clinical and Molecular Hepatology, 24*(2), 100.

Chang, B., Sang, L., Tong, J., Zhang, D., & Wang, B. (2013). The protective effect of VSL#3 on intestinal permeability in a rat model of alcoholic intestinal injury. *BMC Gastroenterology, 13*(1), 151.

Chen, P., Stärkel, P., Turner, J. R., Ho, S. B., & Schnabl, B. (2015). Dysbiosis-induced intestinal inflammation activates tumor necrosis factor receptor I and mediates alcoholic liver disease in mice. *Hepatology, 61*(3), 883–894.

Chen, R., Xu, L., Du, S., Huang, S., Wu, H., Dong, J., Huang, J., Wang, X., Feng, W., & Chen, Y. (2016). *Lactobacillus rhamnosus* GG supernatant promotes intestinal barrier function, balances T reg and T H 17 cells and ameliorates hepatic injury in a mouse model of chronic-binge alcohol feeding. *Toxicology Letters, 241*, 103–110.

Chen, Y., Yang, F., Lu, H., Wang, B., Chen, Y., Lei, D., & Li, L. (2011). Characterization of fecal microbial communities in patients with liver cirrhosis. *Hepatology, 54*(2), 562–572.

Crabb, D. W., Matsumoto, M., Chang, D., & You, M. (2004). Overview of the role of alcohol dehydrogenase and aldehyde dehydrogenase and their variants in the genesis of alcohol-related pathology. *Proceedings of the Nutrition Society, 63*(1), 49–63.

Dubinkina, V. B., Tyakht, A. V., Odintsova, V. Y., Yarygin, K. S., Kovarsky, B. A., Pavlenko, A. V., & Taraskina, A. Y. (2017). Links of gut microbiota composition with alcohol dependence syndrome and alcoholic liver disease. *Microbiome, 5*(1), 141.

Dunn, W., & Shah, V. H. (2016). Pathogenesis of alcoholic liver disease. *Clinics in Liver Disease, 20*(3), 445–456.

Engen, P. A., Green, S. J., Voigt, R. M., Forsyth, C. B., & Keshavarzian, A. (2015). Alcohol effects on the composition of intestinal microbiota. *Alcohol Research, 37*(2), 223–236.

Ferrere, G., Wrzosek, L., Cailleux, F., Turpin, W., Puchois, V., Spatz, M., & Hugot, C. (2017). Fecal microbiota manipulation prevents dysbiosis and alcohol-induced liver injury in mice. *Journal of Hepatology, 66*(4), 806–815.

Hao, L., Sun, Q., Zhong, W., Zhang, W., Sun, X., & Zhou, Z. (2018). Mitochondria-targeted ubiquinone (MitoQ) enhances acetaldehyde clearance by reversing alcohol-induced posttranslational modification of aldehyde dehydrogenase 2: A molecular mechanism of protection against alcoholic liver disease. *Redox Biology, 14*, 626–636.

Hong, M., Kim, S. W., Han, S. H., Kim, D. J., Suk, K. T., Kim, Y. S., ... Ham, Y. L. (2015). Probiotics (*Lactobacillus rhamnosus* R0011 and *acidophilus* R0052) reduce the expression of Toll-Like Receptor 4 in mice with alcoholic liver disease. *Plos One, 10*(2).

Johansson, M. E., Sjövall, H., & Hansson, G. C. (2013). The gastrointestinal mucus system in health and disease. *Nature Reviews Gastroenterology & Hepatology, 10*(6), 352.

Kim, W. G., Kim, H. I., Kwon, E. K., Han, M. J., & Kim, D. H. (2018). *Lactobacillus plantarum* LC27 and *Bifidobacterium longum* LC67 mitigate alcoholic steatosis in mice by inhibiting LPS-mediated NF-κB activation through restoration of the disturbed gut microbiota. *Food & Function, 9*(8), 4255–4265.

Kirpich, I. A., Solovieva, N. V., Leikhter, S. N., Shidakova, N. A., Lebedeva, O. V., Sidorov, P. I., & McClain, C. J. (2008). Probiotics restore bowel flora and improve liver enzymes in human alcohol-induced liver injury: A pilot study. *Alcohol, 42*(8), 675–682.

Kosnicki, K. L., Penprase, J. C., Cintora, P., Torres, P. J., Harris, G. L., Brasser, S. M., & Kelley, S. T. (2019). Effects of moderate, voluntary ethanol consumption on the rat and human gut microbiome. *Addiction Biology, 24*(4), 617–630.

Leclercq, S., Matamoros, S., Cani, P. D., Neyrinck, A. M., Jamar, F., Stärkel, P., & Verbeke, K. (2014). Intestinal permeability, gut-bacterial dysbiosis, and behavioral markers of alcohol-dependence severity. *Proceedings of the National Academy of Sciences, 111*(42), E4485–E4493.

Leung, T. M., & Nieto, N. (2013). CYP2E1 and oxidant stress in alcoholic and non-alcoholic fatty liver disease. *Journal of Hepatology, 58*(2), 395–398.

Li, F., Duan, K., Wang, C., McClain, C., & Feng, W. (2016). Probiotics and alcoholic liver disease: Treatment and potential mechanisms. *Gastroenterology Research and Practice, 2016*, 1–11.

Llopis, M., Cassard, A., Wrzosek, L., Boschat, L., Bruneau, A., Ferrere, G., & Le Roy, T. (2016). Intestinal microbiota contributes to individual susceptibility to alcoholic liver disease. *Gut, 65*(5), 830–839.

Loguercio, C., Federico, A., Tuccillo, C., Terracciano, F., D'Auria, M. V., De Simone, C., & Blanco, C. D. V. (2005). Beneficial effects of a probiotic VSL#3 on parameters of liver dysfunction in chronic liver diseases. *Journal of Clinical Gastroenterology, 39*(6), 540–543.

Lu, J., Lyu, Y., Li, M., Sun, J., Huang, Z., Lu, F., & Lu, Z. (2018). Alleviating acute alcoholic liver injury in mice with Bacillus subtilis co-expressing alcohol dehydrogenase and acetaldehyde dehydrogenase. *Journal of Functional Foods, 49*, 342–350.

Marotta, F., Barreto, R., Wu, C., Naito, Y., Gelosa, F., Lorenzetti, A., Yoshioka, W., & Fesce, E. (2005). Experimental acute alcohol pancreatitis-related liver damage and endotoxemia: Synbiotics but not metronidazole have a protective effect. *Chinese Journal of Digestive Diseases, 6*(4), 193–197.

Mathurin, P., Deng, Q. G., Keshavarzian, A., Choudhary, S., Holmes, E. W., & Tsukamoto, H. (2000). Exacerbation of alcoholic liver injury by enteral endotoxin in rats. *Hepatology, 32*(5), 1008–1017.

Minemura, M., & Shimizu, Y. (2015). Gut microbiota and liver diseases. *World Journal of Gastroenterology, 21*(6), 1691.

Mortensen, B., Murphy, C., O'Grady, J., Lucey, M., Elsafi, G., Barry, L., ... Eklund, A. C. (2019). *Bifidobacterium breve* Bif195 protects against small-intestinal damage caused by acetylsalicylic acid in healthy volunteers. *Gastroenterology*.

Mutlu, E. A., Gillevet, P. M., Rangwala, H., Sikaroodi, M., Naqvi, A., Engen, P. A., & Keshavarzian, A. (2012). Colonic microbiome is altered in alcoholism. *American Journal of Physiology-Gastrointestinal and Liver Physiology, 302*(9), G966–G978.

Rehm, J., Samokhvalov, A. V., & Shield, K. D. (2013). Global burden of alcoholic liver diseases. *Journal of Hepatology, 59*(1), 160–168.

Reynolds, J. M., Martinez, G. J., Chung, Y., & Dong, C. (2012). Toll-like receptor 4 signaling in T cells promotes autoimmune inflammation. *Proceedings of the National Academy of Sciences, 109*(32), 13064–13069.

Schnabl, B., & Brenne, D. A. (2014). Interactions between the intestinal Microbiome and liver diseases. *Gastroenterology, 146*(6), 1513–1524.

Segawa, S., Wakita, Y., Hirata, H., & Watari, J. (2008). Oral administration of heat-killed *Lactobacillus brevis* SBC8803 ameliorates alcoholic liver disease in ethanol-containing diet-fed C57BL/6N mice. *International Journal of Food Microbiology, 128*(2), 371–377.

Stickel, F., Moreno, C., Hampe, J., & Morgan, M. Y. (2017). The genetics of alcohol dependence and alcohol-related liver disease. *Journal of Hepatology, 66*(1), 195–211.

Tian, F., Chi, F., Wang, G., Liu, X., Zhang, Q., Chen, Y., & Chen, W. (2015). Lactobacillus rhamnosus CCFM1107 treatment ameliorates alcohol-induced liver injury in a mouse model of chronic alcohol feeding. *Journal of Microbiology, 53*(12), 856–863.

Tian, X., Yu, Z., Feng, P., Ye, Z., Li, R., Liu, J., & Li, X. (2019). *Lactobacillus plantarum* TW1-1 alleviates diethylhexylphthalate-induced testicular damage in mice by modulating gut microbiota and decreasing inflammation. *Frontiers in Cellular and Infection Microbiology, 9*, 221.

Tuomisto, S., Pessi, T., Collin, P., Vuento, R., Aittoniemi, J., & Karhunen, P. J. (2014). Changes in gut bacterial populations and their translocation into liver and ascites in alcoholic liver cirrhotics. *BMC Gastroenterology, 14*(1), 40.

Van Beek, A. A., Hoogerland, J. A., Belzer, C., De Vos, P., De Vos, W. M., Savelkoul, H. F. J., & Leenen, P. J. M. (2015). Interaction of mouse splenocytes and macrophages with bacterial strains in vitro: the effect of age in the immune response. *Beneficial Microbes, 7*(2), 275–287.

Wang, Y., Kirpich, I., Liu, Y., Ma, Z., Barve, S., McClain, C. J., & Feng, W. (2011). *Lactobacillus rhamnosus* GG treatment potentiates intestinal hypoxia-inducible factor, promotes intestinal integrity and ameliorates alcohol-induced liver injury. *The American Journal of Pathology, 179*(6), 2866–2875.

Wang, Y., Liu, Y., Kirpich, I., Ma, Z., Wang, C., Zhang, M., & Feng, W. (2013). *Lactobacillus rhamnosus* GG reduces hepatic TNFα production and inflammation in chronic alcohol-induced liver injury. *The Journal of Nutritional Biochemistry, 24*(9), 1609–1615.

Wang, Y., Liu, Y., Sidhu, A., Ma, Z., McClain, C., & Feng, W. (2012). *Lactobacillus rhamnosus* GG culture supernatant ameliorates acute alcohol-induced intestinal permeability and liver injury. *American Journal of Physiology-Gastrointestinal and Liver Physiology, 303*(1), G32–G41.

Yan, A. W., Fouts, D. E., Brandl, J., Stärkel, P., Torralba, M., Schott, E., & Schnabl, B. (2011). Enteric dysbiosis associated with a mouse model of alcoholic liver disease. *Hepatology, 53*(1), 96–105.

Yano, J. M., Yu, K., Donaldson, G. P., Shastri, G. G., Ann, P., Ma, L., & Hsiao, E. Y. (2015). Indigenous bacteria from the gut microbiota regulate host serotonin biosynthesis. *Cell, 161*(2), 264–276.

Zhang, Z., Zhou, H., Bai, L., Lv, Y., Yi, H., Zhang, L., & Li, R. (2019). Protective effects of probiotics on acute alcohol-induced liver injury in mice through alcohol metabolizing enzymes activation and hepatic TNF-α response reduction. *Journal of Functional Foods, 59*, 234–241.

Zhao, H., Zhao, C., Dong, Y., Zhang, M., Wang, Y., Li, F., Li, X., McClain, C., Yang, S., & Feng, W. (2015). Inhibition of miR122a by *Lactobacillus rhamnosus* GG culture supernatant increases intestinal occludin expression and protects mice from alcoholic liver disease. *Toxicology Letters, 234*(3), 194–200.